Mitigation of Magnetic Field under Egyptian 500kV Overhead Transmission Line

Adel Z. El Dein

***Abstract*—The paper presents an efficient way to mitigate the magnetic field resulting from the three-phase 500kV single circuit high voltage transmission line existing in Egypt, by using a passive loop conductor. The aim of this paper is to reduce the amount of land required as rights-of-way (ROW). The paper used an accurate method for the evaluation of 50Hz magnetic field produced by overhead transmission lines. This method is based on the matrix formalism of multiconductor transmission lines (MTL). This method obtained a correct evaluation of all the currents flowing in the MTL structure, including the currents in the subconductors of each phase bundle, the currents in the ground wires, the currents in the mitigation loop, and also the earth return currents. Furthermore, the analysis also incorporates the effect of the conductors sag between towers, and the effect of sag variation with the temperature on the calculated magnetic field. Good results have been obtained and passive loop conductor design parameters have been recommended for this system at ambient temperature (35^{o}C).**

***Index Terms*—Magnetic Field, Mitigation loop, Right-of-way, Transmission lines**

I. Introduction

THE rabid increase in HV transmission lines and irregular population areas near the manmade sources of electrical and magnetic fields, in Egypt, needs a suggestion of methods to minimize or eliminate the effect of magnetic and electrical fields on human begins in Egyptian environmental areas especially in irregular areas. Public concern about magnetic field effects on human safety has triggered a wealth of research efforts focused on the evaluation of magnetic fields produced by power lines [1], [2]. Studies include the design of new compact transmission line configurations; the inclusion of auxiliary single or double lops for magnetic field mitigation in already existing power lines; the consideration of series-capacitor compensation schemes for enhancing magnetic field mitigation; the reconfiguration of lines to high phase operation, etc [3]-[5]. However, many of the studies presented that deal with power lines make use of certain simplifying assumptions that, inevitably, give rise to inaccurate results in the computed magnetic fields. Ordinary simplifications include neglecting the earth currents, neglecting the ground wires, replacing bundle phase conductors with equivalent single conductors, and replacing actual sagged conductors with average height Horizontal conductors. These assumptions result in a model where magnetic fields are distorted from those produced in reality [6], [7]. In this paper, a matrix-based MTL model [8], where the effects of earth currents, ground wire currents and mitigation loop current are taken into account, is used; moreover, actual bundle conductors and conductors' sag at various temperatures are taken into consideration. The results from this method without mitigation loop are compared with those produced from the common practice method [6], [7] for Magnetic field calculation where the power transmission lines are straight horizontal wires of infinite length, parallel to a flat ground and parallel with each other. Then the optimal parameters of the mitigation loop design for Egyptian 500kV overhead transmission line are obtained.

Manuscript received February 16, 2010. Paper no. ICEEE_21. The author is with the Department of Electrical Engineering, High Institute of Energy, South Valley University, Aswan 81258, Egypt (e-mail:azeinm2001@hotmail.com).

II. Computation of System Currents

The MTL technique is used in this paper for the simple purpose of deriving the relationship among the line currents of an overhead power line. This method is explained in [8], this paper reviews and extends this method for Egyptian 500kV overhead transmission line, with an other formula for the conductors' sag, taken into account the effect of temperature on the sag configuration [9]. The first step required to conduct a correct analysis consists in determination of all system currents based on prescribed phase-conductor currents I_p:

$$I_p = \begin{bmatrix} I_1 & ; & I_2 & ; & I_3 \end{bmatrix} \tag{1}$$

Consider the frequency-domain transmission line matrix equations for non-uniform MTLs (allowing the inclusion of the sag effect)

$$-dV/dz = Z`(\omega, z)I \tag{2a}$$

$$-dI/dz = Y`(\omega, z)V \tag{2b}$$

Where $Z`$ and $Y`$, denote the per-unit-length series-impedance and shunt-admittance matrices, respectively ,V and I are complex column matrices collecting the phasors associated with all of the voltages and currents of the line conductors, respectively.

$$V = \begin{bmatrix} [V_a]_{1\times n_p} \\ [V_b]_{1\times n_p} \\ [V_c]_{1\times n_p} \\ [V_G]_{1\times n_G} \\ [V_L]_{1\times n_L} \end{bmatrix} \quad \text{and} \quad I = \begin{bmatrix} [I_a]_{1\times n_p} \\ [I_b]_{1\times n_p} \\ [I_c]_{1\times n_p} \\ [I_G]_{1\times n_G} \\ [I_L]_{1\times n_L} \end{bmatrix} \tag{3}$$

In (3), subscripts *a, b*, and *c* refer to the partition of phase bundles into three sub-conductor sets. Subscript *G* refers to ground wires and *L* subscript refers to the mitigation loop. In (3) n_p, n_G, and n_L denote, the number of phase bundles, the number of ground wires, and the number of conductors in the mitigation loop, respectively, for the Egyptian 500kV overhead transmission line it is seen that: $n_p = 3$, $n_G = 2$, and $n_L = 2$ as it is proposed in this paper. Since the separation of the electric and magnetic effects is an adequate approach for

ISBN: 978-988-18210-7-2
ISSN: 2078-0958 (Print); ISSN: 2078-0966 (Online)

quasistationary regimes (50Hz), where wave-propagation phenomena are negligible, all system currents are assumed to be Z independent. This means the transversal displacement currents among conductors are negligible or, in other words, (2b) equates to zero and only *Z`* values are needed to calculate. Since the standard procedure for computing *Z`* in (2a) has been established elsewhere [10]-[12], details will not be revealed here and thus only a brief summary is presented.

$$Z` = j\omega L + Z_E + Z_{skin} \tag{4}$$

The external-inductance matrix is a frequency-independent real symmetric matrix whose entries are:

$$L_{kk} = (\mu_o / 2\pi)\ln(2y_k / r_k) \tag{5a}$$

$$L_{kk} = \frac{\mu_o}{4\pi}\ln\frac{(y_i + y_k)^2 + (x_i + x_k)^2}{(y_i - y_k)^2 + (x_i + x_k)^2} \tag{5b}$$

Where r_k denotes conductor radius, and y_k and x_k denote the vertical and horizontal coordinates of conductor *k*. Matrix Z_E , the earth impedance correction, is a frequency dependent complex matrix whose entries can be determine using Carson's theory or, alternatively, the Dubanton complex ground plane approach [10]-[12]. The entries of Z_E are defined as:

$$(Z_E)_{kk} = (j\omega\mu_o / 2\pi)\ln\left(1 + \overline{\mathrm{P}} / y_k\right) \tag{6a}$$

$$(Z_E)_{ik} = j\omega\frac{\mu_o}{4\pi}\ln\left(\frac{(y_i + y_k + 2\overline{\mathrm{P}})^2 + (x_i - x_k)^2}{(y_i - y_k)^2 + (x_i - x_k)^2}\right) \tag{6b}$$

where $\overline{\mathrm{P}}$, the complex depth, is given by $\overline{\mathrm{P}} = (j\omega\mu_o / \rho)^{-1/2}$ with ρ denoting the earth resistivity. Matrix Z_{skin} is a frequency-dependent complex diagonal matrix whose entries can be determined by using the skin-effect theory results for cylindrical conductors [7].
For low-frequency situations, it will be:

$$(Z_{skin})_{kk} = (R_{dc})_k + j\omega(\mu_o / 8\pi) \tag{7}$$

Where $(R_{dc})_k$ denotes the per-unit-length dc resistance of conductor *k*. Due to the line conductors' sag between towers; y_k will be a function on the distance *z* between the two towers, also the entries for *L* and Z_E, defined in (5) and (6), vary along the longitudinal coordinate *z*. The exact shape of a conductor suspended between two towers of equal height can be described by such parameters; as the distance between the points of suspension span, *d*, the sag of the conductor, *S*, the height of the lowest point above the ground, *h*, and the height of the highest point above the ground, *hm*. These parameters can be used in different combinations [13], [14]. Fig. (1) depicts the basic catenary geometry for a single-conductor line, this geometry is described by:

$$y_k = h_k + 2\alpha_k \sinh^2(z/(2\alpha_k)) \tag{8}$$

Where α_k is the solution of the transcendental equation: $2[(hm_k - h_k)/d_k]u_k = \sinh^2(u_k)$, for conductor *k*; with $u_k = d_k/(4\alpha_k)$. The parameter α_k is also associated with the mechanical parameters of the line: $\alpha_k = (T_h)_k / w_k$ where $(T_h)_k$ is the conductor tension at mid-span and w_k is weight per unit length of the conductor *k*.

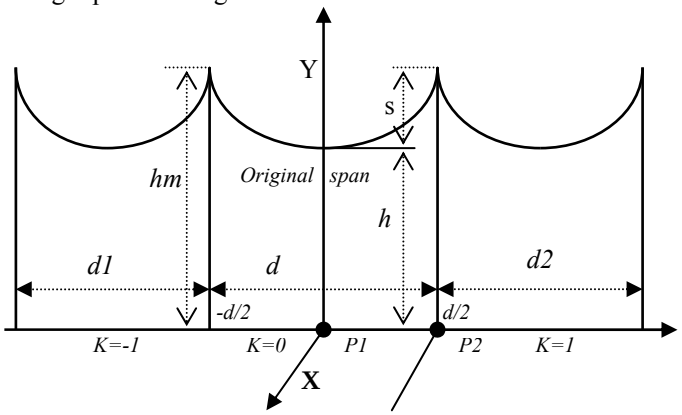

Fig. 1. Linear dimensions which determine parameters of the catenary.

Consider a mitigation loop of length *l*, is present, where *l* is a multiple of the span length *d*. The line section under analysis has its near end at *-l/2* and its far end at *l/2*.
The integration of (2a) from *z = -l/2* to *z = l/2* gives:

$$V_{near} - V_{far} = I\int_{-l/2}^{l/2} Z`(z)dz \tag{9a}$$

Equation (9a) can be written explicitly, in partitioned form, as:

$$\begin{bmatrix}\Delta V_a\\ \Delta V_b\\ \Delta V_c\\ \Delta V_G\\ \Delta V_L\end{bmatrix} = \begin{bmatrix}Z_{aa} & Z_{ab} & Z_{ac} & Z_{aG} & Z_{aL}\\ Z_{ba} & Z_{bb} & Z_{bc} & Z_{bG} & Z_{bL}\\ Z_{ca} & Z_{cb} & Z_{cc} & Z_{cG} & Z_{cL}\\ Z_{Ga} & Z_{Gb} & Z_{Gc} & Z_{GG} & Z_{GL}\\ Z_{La} & Z_{Lb} & Z_{Lc} & Z_{LG} & Z_{LL}\end{bmatrix}\begin{bmatrix}I_a\\ I_b\\ I_c\\ I_G\\ I_L\end{bmatrix} \tag{9b}$$

The computation of the bus impedance *Z* in equation (9) is performed using the following formula:

$$Z = \int_{-l/2}^{l/2} Z`(z)dz \tag{10}$$

Where values for *Z`* are evaluated from equations (4-7) considering the conductors' heights given by (8). The two-conductor mitigation loop is closed and may include or not a series capacitor of impedance Z_c [5]. In any case, the submatrix I_L in (3) has the form:

$$I_L = \begin{bmatrix} I_{L1} & ; & I_{L2}\end{bmatrix} = \mathrm{I}_L S^T \tag{11}$$

where; $S = \begin{bmatrix}1 & -1\end{bmatrix}$

By using the boundary conditions at both the near and far end of the line section, the voltage drop in the mitigation loop will be:

ISBN: 978-988-18210-7-2
ISSN: 2078-0958 (Print); ISSN: 2078-0966 (Online)

$$\Delta V_L = \begin{bmatrix} \Delta V_{L1} \\ \Delta V_{L2} \end{bmatrix} = \begin{bmatrix} V_{L1} \\ V_{L2} \end{bmatrix}_{near} - \begin{bmatrix} V_{L1} \\ V_{L2} \end{bmatrix}_{far} = \begin{bmatrix} \Delta V_{L1} \\ \Delta V_{L1} + Z_c \mathrm{I}_L \end{bmatrix}$$

which can be written as:

$$S\Delta V_L = \Delta V_{L1} - \Delta V_{L2} = -Z_c \mathrm{I}_L \tag{12}$$

Where I_L is the loop current, and $Z_c = jX_s = 1/(j\omega C_s)$ is the impedance of the series capacitor included in the loop.

Using (12), the fifth equation contained in (9b) allows for the evaluation of the currents flowing in the mitigation loop.

$$I_L = [\mathrm{I}_L \quad ; \quad -\mathrm{I}_L] \tag{13}$$
$$= -\underbrace{YS^T SZ_{La}}_{K_{La}} I_a - \underbrace{YS^T SZ_{Lb}}_{K_{Lb}} I_b - \underbrace{YS^T SZ_{Lc}}_{K_{Lc}} I_c - \underbrace{YS^T SZ_{LG}}_{K_{LG}} I_G$$

Where ; $Y = 1/(Z_c + SZ_{LL}S^T)$

Taking into account that the conductors belonging to given phase bundle are bonded to each other, and that ground wires are bonded to earth (tower resistances neglected), that result in:

$$\Delta V_a = \Delta V_b = \Delta V_c \text{ and } \Delta V_G = 0$$

By using $\Delta V_G = 0$ in the fourth equation contained in (9b) and using equation (13), the ground wire will be:

$$I_G = \underbrace{Y_G(Z_{Ga} - Z_{GL}K_{La})}_{K_{Ga}} I_a + \underbrace{Y_G(Z_{Gb} - Z_{GL}K_{Lb})}_{K_{Gb}} I_b + \underbrace{Y_G(Z_{Gc} - Z_{GL}K_{Lc})}_{K_{Gc}} I_c \tag{14}$$

Where; $Y_G = (Z_{GL}K_{LG} - Z_{GG})^{-1}$

Next, by using (13) and (14), I_L and I_G can be eliminated in (9b), yielding a reduced-order matrix problem:

$$\begin{bmatrix} \Delta V_a \\ \Delta V_b \\ \Delta V_c \end{bmatrix} = \begin{bmatrix} \hat{Z}_{aa} & \hat{Z}_{ab} & \hat{Z}_{ac} \\ \hat{Z}_{ba} & \hat{Z}_{bb} & \hat{Z}_{bc} \\ \hat{Z}_{ca} & \hat{Z}_{cb} & \hat{Z}_{cc} \end{bmatrix} \begin{bmatrix} I_a \\ I_b \\ I_c \end{bmatrix} \tag{15}$$

where ; $\hat{Z}_{aa} = Z_{aa} + Z_{aG}K_{Ga} - Z_{aL}(K_{La} + K_{LG}K_{Ga})$

$$\hat{Z}_{ab} = Z_{ab} + Z_{aG}K_{Gb} - Z_{aL}(K_{Lb} + K_{LG}K_{Gb})$$
$$\hat{Z}_{ac} = Z_{ac} + Z_{aG}K_{Gc} - Z_{aL}(K_{Lc} + K_{LG}K_{Gc})$$
$$\hat{Z}_{ba} = Z_{ba} + Z_{bG}K_{Ga} - Z_{bL}(K_{La} + K_{LG}K_{Ga})$$
$$\hat{Z}_{bb} = Z_{bb} + Z_{bG}K_{Gb} - Z_{bL}(K_{Lb} + K_{LG}K_{Gb})$$
$$\hat{Z}_{bc} = Z_{bc} + Z_{bG}K_{Gc} - Z_{bL}(K_{Lc} + K_{LG}K_{Gc})$$
$$\hat{Z}_{ca} = Z_{ca} + Z_{cG}K_{Ga} - Z_{cL}(K_{La} + K_{LG}K_{Ga})$$
$$\hat{Z}_{cb} = Z_{cb} + Z_{cG}K_{Gb} - Z_{cL}(K_{Lb} + K_{LG}K_{Gb})$$
$$\hat{Z}_{cc} = Z_{cc} + Z_{cG}K_{Gc} - Z_{cL}(K_{Lc} + K_{LG}K_{Gc})$$

The relationship between I_a, I_b and I_c is obtained from (15) by making $\Delta V_a = \Delta V_b = \Delta V_c$ and by using $I_a + I_b + I_c = I_p$. Then the following relations are obtained

$$I_a = KK_{ac}(KK_{ac} + K_{bc} + 1)^{-1} I_p \tag{16a}$$
$$I_b = KK_{bc}(KK_{ac} + K_{bc} + 1)^{-1} I_p \tag{16b}$$
$$I_c = (KK_{ac} + K_{bc} + 1)^{-1} I_p \tag{16c}$$

Where ; $KK_{ac} = KK_{ab}KK_{bc} + KK_{ac}$

$$K_{ab} = Y_a(\hat{Z}_{bb} - \hat{Z}_{ab}) \; ; \; K_{ac} = Y_a(\hat{Z}_{bc} - \hat{Z}_{ac})$$
$$Y_a = (\hat{Z}_{aa} - \hat{Z}_{ba})^{-1} \; ; \; K_{bc} = (K_{bc1})^{-1} K_{cb1}$$
$$K_{bc1} = \hat{Z}_{ca}K_{ab} + \hat{Z}_{cb} - \hat{Z}_{ba}K_{ab} - \hat{Z}_{bb}$$
$$K_{cb1} = \hat{Z}_{ba}K_{ac} + \hat{Z}_{bc} - \hat{Z}_{ca}K_{ac} - \hat{Z}_{cc}$$

Once I_P is given, all of the overhead conductor currents I_a, I_b, I_c, I_G and I_L can be evaluated, step after step using (16),(14), and (13)

The net current returning through the earth I_E is the complement of the sum of all overhead conductor currents

$$I_E = -\left[\sum_{k=1}^{n_p}(I_a)_k + \sum_{k=1}^{n_p}(I_b)_k + \sum_{k=1}^{n_p}(I_c)_k + \sum_{k=1}^{n_G}(I_G)_k + \sum_{k=1}^{n_L}(I_L)_k\right] \tag{17}$$

The sag of each conductor depends on individual characteristics of the line and environmental conditions. By using the Overhead Cable Sag Calculation Program [15], the sag variation with the temperatures can be calculated as in table (I).

TABLE (I)
TEMPERATURE EFFECT

Temperature	15°C	20°C	25°C	30°C	35°C	40°C	45°C
Sag (m)	7.3	7.8	8.3	8.8	9.3	9.8	10.3

Once all system currents are calculated, the magnetic field at any point, which produced from these currents, can be calculated

III. MAGNETIC FIELD CALCULATIONS

By using the Integration Technique, which explained in details in [13] and reviewed here, the magnetic field produced by a multiphase conductors (*M*), and their images, in support structures at any point $P(x_o,y_o,z_o)$ can be obtained by using the Biot-Savart law as [7], [13]:

$$H_o = \frac{1}{4\pi}\sum_{K=1}^{M}\sum_{n=-N}^{N}\int_{-d/2}^{d/2}\left[(H_x)_k\vec{a}_x + (H_y)_k\vec{a}_y + (H_z)_k\vec{a}_z\right]dz \tag{18}$$

Where:

$$(H_x)_k = I_k\left[(z - z_o + nd)\sinh(\frac{z}{\alpha_k}) - (y_k - y_o)\right]/d_k -$$
$$I_k\left[(z - z_o + nd)\sinh(\frac{z}{\alpha_k}) - (y_k + y_o + 2\overline{\mathrm{P}})\right]/d`_k \tag{19}$$

$$(H_y)_k = I_k(x_k - x_o)/d_k - I_k(x_k - x_o)/d`_k \tag{20}$$

ISBN: 978-988-18210-7-2
ISSN: 2078-0958 (Print); ISSN: 2078-0966 (Online)

$$(H_z)_k = I_k[-(x_k - x_o)\sinh(\frac{z}{\alpha_k})/d_k + (x_k - x_o)\sinh(\frac{z}{\alpha_k})/d'_k] \quad (21)$$

$$d_k = \left[(x_k - x_o)^2 + (y_k - y_o)^2 + (z - z_o + nd)^2\right]^{3/2} \quad (22)$$

$$d'_k = \left[(x_k - x_o)^2 + (y_k + y_o + 2\bar{P})^2 + (z - z_o + nd)^2\right]^{3/2} \quad (23)$$

The parameter (N) in (18) represents the number of spans to the right and to the left from the generic one.

IV. Results and Discussion

The data used in the calculation of the magnetic field intensity at points one meter above ground level (field points), under Egyptian 500kV TL single circuit are as presented in table II.

The phase-conductor currents are defined by a balanced direct-sequence three-phase set of 50Hz sinusoidal currents, with 2-kA rms, that is

$$I_p = 2\left[1 \quad ; \quad e^{-j2\pi/3} \quad ; \quad e^{j2\pi/3}\right] \text{kA} \quad (24)$$

Fig. (2) shows the effect of the number of spans (N) on the calculated magnetic field intensity. It is noticed that, when the magnetic field intensity calculated at point P1 (Fig.1) and a distance away from the center phase, the effect of the spans' number is very small due to the symmetry of the spans around the calculation points, as explained in Fig. (1), where the contributions of the catenaries *d1* and *d2* are equal and smaller than the contribution of the catenary *d*, as they far from the field points. But when the magnetic field intensity calculated at point P2 (Fig.1) and a distance away from the center phase, the effect of the spans' number is of great effect (double), that due to the contribution of the catenary *d2* which produced the same magnetic field intensity as the original span *d* in this case as explained in Fig. (1), and of course the catenary *d1* have a small contribution in the calculated values of the magnetic field intensities in this case.

TABLE (II)
Characteristics of 500KV Line Conductors

Conductor number	Radius (mm)	X-Coordinate (m)	Y-Coordinate (m)	R_{dc} at 20°C (Ω/km)
1a	15.3	-13.425	22.13	0.0511
1b	15.3	-12.975	22.13	0.0511
1c	15.3	-13.2	21.74	0.0511
2a	15.3	-0.225	24.48	0.0511
2b	15.3	0.225	24.48	0.0511
2c	15.3	0	24.09	0.0511
3a	15.3	12.975	22.13	0.0511
3b	15.3	13.425	22.13	0.0511
3c	15.3	13.2	21.74	0.0511
G1	5.6	-8	30	0.564
G2	5.6	8	30	0.564
L1	11.2	-13.2	17	0.1168
L2	11.2	13.2	17	0.1168

Fig. (3) shows the effects of the temperatures on the configuration of overhead transmission line conductors (sag) and hence on the calculated magnetic field intensity by using 3D integration technique with MTL technique. It is seen that as the sag increased with the increase in the temperatures (as indicated in table (I)), the magnetic field intensity also increased. Fig. (4) shows the comparison between the magnetic filed calculated with both 2D straight line technique where the average conductors' heights are used, and 3D integration technique with MTL technique. It is seen that the observed maximum error of -23.2959% (at point P1) and 49.877% at (point P2) is mainly due to the negligence of the sage effect on the conductors.

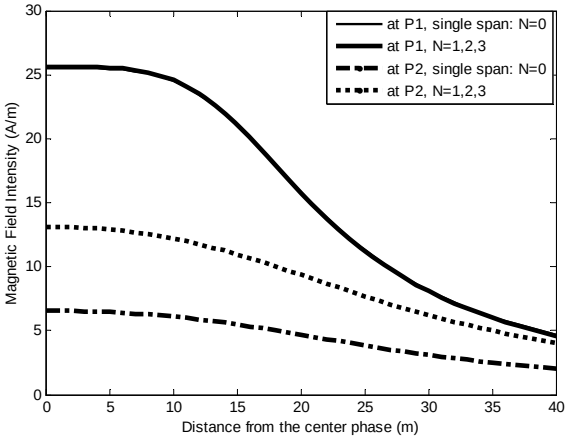

Fig. 2. The effect of the spans' numbers on the magnetic field intensity.

Fig. (5) shows the comparison between the magnetic field intensity calculated by using 3D integration technique with MTL technique with and without ground wires and with and without the short circuit mitigation loop. It is seen that, the observed maximum reduction of 1.9316% (at point P1) and 2.469% (at point P2) is mainly due to the negligence of the ground wires. It is seen that with the short circuit mitigation loop placed 5m below beneath the outer phase conductors, the magnetic field intensity reduced to a significant values, maximum reduction of 25.7063% (at point P1) and 30.1525% (at point P2). The magnetic field intensity can be reduced further by inserting an appropriately chosen series capacitor in the mitigation loop, in order to determine the optimal capacitance Cs of the capacitor to be inserted in the mitigation loop, the magnetic field intensity calculated at point one meter above ground surface under center phase, considering different values of Zc where Zc=jXs, with the reactance Xs varies from -2Ω to 0.

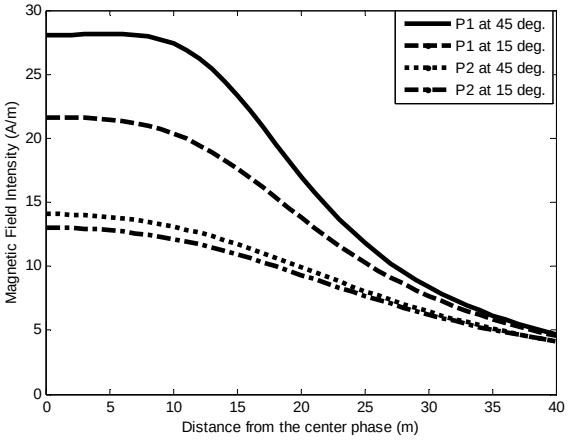

Fig. 3. The effect of the temperatures on the magnetic field intensity.

ISBN: 978-988-18210-7-2
ISSN: 2078-0958 (Print); ISSN: 2078-0966 (Online)

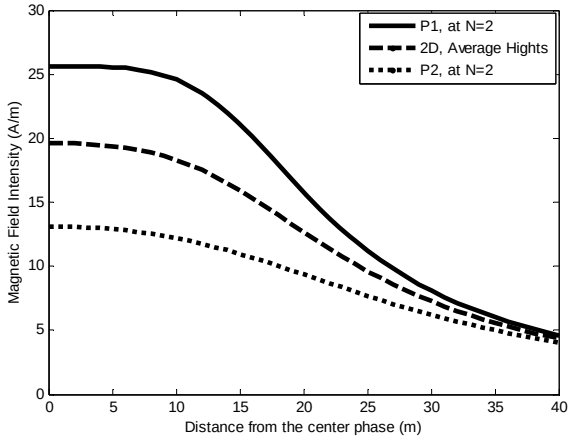

Fig. 4. Comparison between the 2D average heights and 3D integration technique results.

Fig. (6) shows the graphical results of the effect of the reactance Xs, inserted in the mitigation loop, on the magnetic field intensity, from which it is seen that the optimal situation (minimum value of magnetic field intensity) is characterized by Cs=4.897mF, and worst situation (maximum value of magnetic field intensity) is characterizes by Cs=2.358 mF.

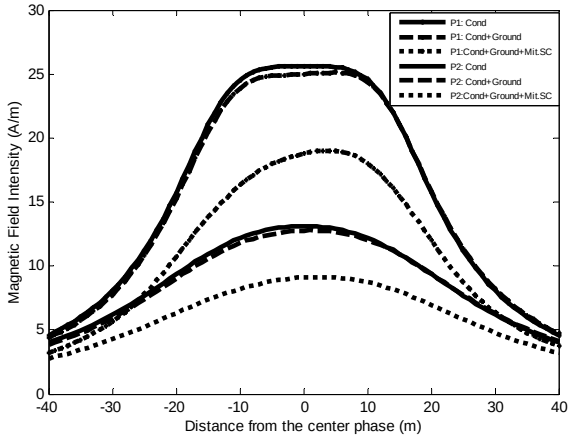

Fig. 5. Comparison between the calculated magnetic field intensity values result from the conductors only, the conductors and ground wires, and the conductors, ground wires and short circuit mitigation loop.

Tables (III) and (IV) depict the effect of the mitigation loop height on the calculated magnetic field intensity at points P1 and P2, respectively, when the mitigation loop spacing is 26.4m (exactly under the outer phases). It is seen that the optimal height is one meter below the outer phase conductors when the mitigation loop is short circuited and about one meter above the outer phase conductors when an optimal capacitance inserted in the mitigation loop. Tables (V) and (VI) depict the effect of the mitigation loop spacing on the calculated magnetic field intensity at points P1 and P2, respectively, when the mitigation loop height is 21m. It is seen that the optimal spacing is the outer phase conductors spacing. Figure (7) shows the comparison between the calculated magnetic field intensity values result from; the conductors, ground wires and short circuit mitigation loop; and the conductors, ground wires and mitigation loop with optimal capacitance and optimal parameters obtained from tables (III), (IV), (V) and (VI). It is seen that the magnetic field intensity decreased further more, maximum reduction of 8.0552% (at point P1) and 19.5326% (at point P2).

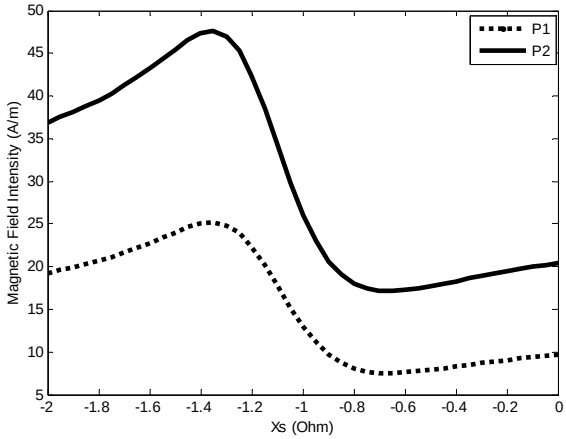

Fig. 6. The effect of the reactance Xs, inserted in the mitigation loop, on the magnetic field intensity.

TABLE (III)
THE EFFECT OF THE MITIGATION LOOP HEIGHTS ON THE CALCULATED MAGNETIC FIELD INTENSITY AT POINT (P1) AND 26.4M MITIGATION LOOP SPACING.

Height of Mitigation loop		Magnetic Field (A/m) at P1 at distance from center phase equals:				
		-15m	-10m	0m	10m	15m
18m	Short Circuit	15.03	17.77	20.83	19.74	16.83
	With Opt. C.	9.42	10.80	17.52	18.84	16.1
19m	Short Circuit	14.93	17.76	20.45	19.71	16.78
	With Opt. C.	8.88	10.82	17.12	18.77	15.98
20m	Short Circuit	14.64	17.52	19.94	19.49	16.57
	With Opt. C.	8.13	10.43	16.63	18.64	15.84
21m	Short Circuit	14.19	17.06	19.26	19.01	16.13
	With Opt. C.	7.01	9.56	15.87	18.15	15.40
23m	Short Circuit	14.10	17.01	19.00	19.31	16.43
	With Opt. C.	7.07	9.86	16.35	19.16	16.41
24m	Short Circuit	16.64	19.80	21.19	21.33	18.24
	With Opt. C.	11.46	14.13	17.97	19.79	16.96
25m	Short Circuit	18.03	21.33	22.46	22.53	19.31
	With Opt. C.	13.95	16.87	19.55	20.85	17.91
26m	Short Circuit	18.95	22.34	23.34	23.35	20.04
	With Opt. C.	15.70	18.764	20.82	21.80	18.74
27m	Short Circuit	19.61	23.08	24.00	23.96	20.58
	With Opt. C.	16.98	20.16	21.84	22.58	19.42

TABLE (IV)
THE EFFECT OF THE MITIGATION LOOP HEIGHTS ON THE CALCULATED MAGNETIC FIELD INTENSITY AT POINT (P2) AND 26.4M MITIGATION LOOP SPACING.

Height of Mitigation loop		Magnetic Field (A/m) at P2 at distance from center phase equals:				
		-15m	-10m	0m	10m	15m
18m	Short Circuit	7.97	8.89	9.88	9.43	8.61
	With Opt. C.	5.49	6.28	7.77	7.99	7.44
19m	Short Circuit	7.77	8.7	9.68	9.26	8.44
	With Opt. C.	5.15	5.98	7.53	7.85	7.30
20m	Short Circuit	7.48	8.4	9.37	9.00	8.20
	With Opt. C.	4.67	5.54	7.21	7.64	7.12
21m	Short Circuit	7.09	7.99	8.93	8.61	7.84
	With Opt. C.	3.98	4.88	6.67	7.25	6.76
23m	Short Circuit	6.79	7.71	8.72	8.49	7.72
	With Opt. C.	3.91	4.93	6.98	7.72	7.22
24m	Short Circuit	8.06	9.09	10.06	9.65	8.74
	With Opt. C.	5.52	6.49	8.01	8.30	7.66
25m	Short Circuit	8.76	9.85	10.82	10.32	9.33
	With Opt. C.	6.67	7.68	8.99	9.01	8.25
26m	Short Circuit	9.23	10.37	11.34	10.78	9.74
	With Opt. C.	7.5	8.56	9.76	9.61	8.75
27m	Short Circuit	9.58	10.75	11.73	11.13	10.05
	With Opt. C.	8.13	9.22	10.37	10.09	9.17

ISBN: 978-988-18210-7-2
ISSN: 2078-0958 (Print); ISSN: 2078-0966 (Online)

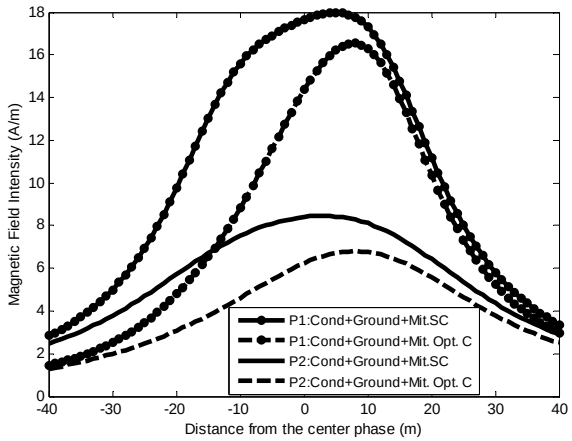

Fig. 7. Comparison between the calculated magnetic field intensity values result from the conductors, ground wires and short circuit mitigation loop; and from the conductors, ground wires and mitigation loop with capacitance of optimal value at optimal height and spacing

TABLE (V)
THE EFFECT OF THE MITIGATION LOOP SPACINGS ON THE CALCULATED MAGNETIC FIELD INTENSITY AT POINT (P1) AND 21M HEIGHT.

Distance of Mitigation loop from the center phase		Magnetic Field (A/m) at P1 at distance from center phase equals:				
		-15m	-10m	0m	10m	15m
5m	Short Circuit	21.54	25.03	24.88	25.56	22.20
	With Opt. C.	20.77	24.07	23.28	24.83	21.75
7.5m	Short Circuit	20.43	23.48	23.24	24.15	21.22
	With Opt. C.	18.65	21.21	20.67	22.73	20.26
10m	Short Circuit	18.35	20.90	21.42	21.98	19.45
	With Opt. C.	14.77	16.58	18.25	20.19	18.01
13.2m	Short Circuit	14.19	17.06	19.26	19.01	16.13
	With Opt. C.	7.01	9.56	15.87	18.15	15.40
15m	Short Circuit	14.57	18.22	20.51	20.19	16.69
	With Opt. C.	7.66	11.28	17.14	19.17	16.12

TABLE (VI)
THE EFFECT OF THE MITIGATION LOOP SPACINGS ON THE CALCULATED MAGNETIC FIELD INTENSITY AT POINT (P2) AND 21M HEIGHT.

Distance of Mitigation loop from the center phase		Magnetic Field (A/m) at P2 at distance from center phase equals:				
		-15m	-10m	0m	10m	15m
5m	Short Circuit	10.69	11.89	12.79	12.17	11.06
	With Opt. C.	10.21	11.32	12.16	11.73	10.72
7.5m	Short Circuit	10.06	11.14	11.96	11.46	10.47
	With Opt. C.	9.01	9.94	10.73	10.57	9.77
10m	Short Circuit	9.01	9.97	10.77	10.38	9.52
	With Opt. C.	7.13	7.93	8.91	9.05	8.44
13.2 m	Short Circuit	7.09	7.99	8.93	8.61	7.84
	With Opt. C.	3.98	4.88	6.67	7.25	6.76
15m	Short Circuit	7.28	8.33	9.41	8.98	8.08
	With Opt. C.	4.34	5.38	7.24	7.69	7.10

V. CONCLUSIONS

Ordinary simplifications, which usually are assuming, in the calculation of the magnetic field under overhead transmission lines, actually result in a model where magnetic fields are distorted from those produced in reality. These simplifications include neglecting the earth currents, neglecting the ground wires, replacing bundle phase conductors with equivalent single conductor, and replacing actual sagged conductors with average height horizontal conductors.

In this paper, the effects of the currents in the subconductors of each phase bundle, the currents in the ground wires, the currents in the mitigation loop, and also the earth return currents; in the calculation of the magnetic field under the 500kV Egyptian overhead transmission line, are investigated by using the MTL technique. Furthermore, the effect of the conductor's sag between towers, and the effect of sag variation with the temperature on the calculated magnetic field is studied. The results from this method without mitigation loop are compared with those produced from the common practice 2-D method.

Finally the passive loop conductor design parameters, for Egyptian 500kV overhead transmission line, are obtained at ambient temperature (35^{o}C).

REFERENCES

[1] Ahmed A. Hossam-Eldin, "Effect of Electromagnetics Fields from Power Lines on Living Organisms" 2001 IEEE 7th International Conference on Solid Dielectrics, June 25-29, Eindhoven, the Netherlands , pp. 438-441

[2] H. Karawia, K. Youssef and A. A. Hossam-Eldin "Measurements and Evaluation of Adverse Health Effects of Electromagnetic Fields from Low Voltage Equipments" MEPCON 2008, Aswan, Egypt, March 12-15 ,PP. 436-440.

[3] A. A. Dahab, F. K. Amoura, and W. S. Abu-Elhaija "Comparison of Magnetic-Field Distribution of Noncompact and Compact Parallel Transmission-Line Configurations" IEEE Transactions on Power Delivery, Vol. 20, No. 3, pp. 2114-2118, July 2005.

[4] J. R. Stewart, S. J. Dale, K. W. Klein "Magnetic Field Reduction Using High Phase order Lines" IEEE Transactions on Power Delivery, Vol. 8, No. 2, April 1993, pp. 628-636.

[5] K. Yamazaki, T. Kawamoto, and H. Fujinami "Requirements for Power Line Magnetic Field Mitigation Using a Passive Loop Conductor" IEEE Transactions on Power Delivery, Vol. 15, No. 2, April 2000, pp. 646-651

[6] R. G. Olsen and P. Wong, "Characteristics of low frequency electric and magnetic fields in the vicinity of electric power lines" IEEE Transactions on Power Delivery, Vol. 7, No. 4, October 1992, pp. 2046-2053.

[7] R. D. Begamudre,"Extra High Voltage AC. Transmission Engineering" third Edition, Book, Chapter 7, pp.172-205, 2006 Wiley Eastern Limited.

[8] J. A. Brandão Faria, and M. E. Almeida "Accurate Calculation of Magnetic-Field Intensity Due to Overhead Power Lines With or Without Mitigation Loops With or Without Capacitor Compensation" IEEE Transactions on Power Delivery, Vol. 22, No. 2, April 2007, pp. 951-959

[9] W. de Villiers, J. H. Cloete, L. M. Wedepohl, and A. Burger "Real-Time Sag Monitoring System for High-Voltage Overhead Transmission Lines Based on Power-Line Carrier Signal Behavior" IEEE Transactions on Power Delivery, Vol. 23, No. 1, January 2008, pp. 389-395

[10] T. Noda,"A Double Logarithmic Approximation of Carson's Ground-Return Impedance", IEEE Transactions on Power Delivery, Vol. 21, No. 1, January 2005, pp. 472-479

[11] A. Ramirez, and F. Uribe," A Broad Range Algorithm for the Evaluation of Carson's Integral", IEEE Transactions on Power Delivery, Vol. 22, No. 2, April 2007, pp. 1188-1193

[12] R. Benato, and R. Caldon," Distribution Line Carrier: Analysis Procedure and Applications to DG", IEEE Transactions on Power Delivery, Vol. 22, No. 1, January 2007, pp. 575-583

[13] Adel Z. El Dein, "Magnetic Field Calculation under EHV Transmission Lines for More Realistic Cases", IEEE Transactions on Power Delivery, Vol. 24, No. 4, pp. 2214-2222, October 2009.

[14] A. V. Mamishev, R. D. Nevels, and B. D. Russell "Effects of Conductor Sag on Spatial Distribution of Power Line Magnetic Field" IEEE Transactions on Power Delivery, Vol.11, No.3, pp.1571-1576, July 1996.

[15] http://infocom.cqu.edu.au/Staff/Michael_O_malley/web/overhead_cable_sag_calculator.html.

ISBN: 978-988-18210-7-2
ISSN: 2078-0958 (Print); ISSN: 2078-0966 (Online)